Quantitative Study of Electroporation-Mediated Molecular Uptake and Cell Viability

Paul J. Canatella,* Joan F. Karr,† John A. Petros,† and Mark R. Prausnitz*‡
Schools of *Chemical and ‡Biomedical Engineering, Georgia Institute of Technology, Atlanta, Georgia 30332, and †Department of Urology, Emory University School of Medicine, Atlanta, Georgia 30322 USA

ABSTRACT Electroporation's use for laboratory transfection and clinical chemotherapy is limited by an incomplete understanding of the effects of electroporation parameters on molecular uptake and cell viability. To address this need, uptake of calcein and viability of DU 145 prostate cancer cells were quantified using flow cytometry for more than 200 different combinations of experimental conditions. The experimental parameters included field strength (0.1–3.3 kV/cm), pulse length (0.05–20 ms), number of pulses (1–10), calcein concentration (10–100 μM), and cell concentration (0.6–23% by volume). These data indicate that neither electrical charge nor energy was a good predictor of electroporation's effects. Instead, both uptake and viability showed a complex dependence on field strength, pulse length, and number of pulses. The effect of cell concentration was explained quantitatively by electric field perturbations caused by neighboring cells. Uptake was shown to vary linearly with external calcein concentration. This large quantitative data set may be used to optimize electroporation protocols, test theoretical models, and guide mechanistic interpretations.

INTRODUCTION

Electroporation has been studied for almost three decades (Chang et al., 1992; Neumann et al., 1989; Lynch and Davey, 1996) and, over that time, has been employed to transport molecules across cell membranes for a wide range of applications, including laboratory gene transfection (Chang et al., 1992; Nickoloff, 1995) and clinical electrochemotherapy (Mir and Orlowski, 1999; Heller et al., 1999). Enhanced uptake is believed to be facilitated by creating transient aqueous pathways in the lipid bilayers of cell membranes. These pathways can be reversible or irreversible depending on the conditions used. Typical conditions employed for cell electroporation range from 1 to 20 kV/cm in strength and 10 μs to 10 ms in duration, depending on cell type (especially size) and application.

Increased molecular uptake into viable cells is the most interesting feature of electroporation and, as such, has received considerable attention. Most studies have quantified uptake in terms of either gene transfection efficiency (Kubiniec et al., 1990; Rols and Teissie, 1990) or percentage of cells electroporated as determined by dye uptake above a detection limit (Neumann et al., 1998; Liang et al., 1988). Although transfection is of practical importance, it is not a direct measure of uptake because gene transfection involves many steps in addition to transport of DNA into a cell. Determining the percentage of cells electroporated provides information more closely related to uptake but does not provide information on the degree of uptake (i.e., the number of molecules transported). A few studies have quantified molecular uptake (and in some cases viability) more directly with measurements made on a large number of individual cells (Bartoletti et al., 1989; Gift and Weaver, 1995; Prausnitz et al., 1993; DeLeo et al., 1996). This was the approach employed in this paper as well.

To understand the dependence of uptake and viability on electroporation parameters and thereby provide mechanistic and practical insight, some studies have measured their dependence on field strength, pulse length, number of pulses, and cell and solute concentration. Based on the limited data sets available in the literature, correlation between transport and electrical charge (Liang et al., 1988; Prausnitz et al., 1994) or energy (Kubiniec et al., 1990; Neumann et al., 1998) has been proposed. Other studies suggest that transport depends on field strength in a more complex manner: 1) no uptake below a quasi-threshold voltage, 2) field-strength-dependent increase in uptake at moderate voltages, and 3) field-strength-independent uptake (i.e., a plateau or saturation) at high voltage (Prausnitz et al., 1993, 1994; Gift and Weaver, 1995). Studies have also shown viability to have a similar dependence on field strength including a threshold, a viability decrease, and then a leveling off to low (i.e., zero) viability levels (Chang et al., 1992).

Building off insight from previous smaller studies of molecular uptake and viability, in this study we examined the effects of electrical and other parameters for over 200 different conditions. We believe this represents the most comprehensive study performed to date. Using these experimental data, we were able to test the following hypotheses: 1) electroporation's effects scale with electrical charge, 2) electroporation's effects scale with electrical energy, 3) electroporated cells generally take up molecules at an inter-

Received for publication 28 February 2000 and in final form 21 November 2000.

J. F. Karr's current address is Cancer Research Program, Department of Health Services, Sacramento, CA 94234-7320.

Address reprint requests to Dr. Mark Prausnitz, School of Chemical Engineering, Georgia Institute of Technology, Atlanta, GA 30332-0100. Tel.: 404-894-5135; Fax: 404-894-2866; E-mail: mark.prausnitz@che.gatech.edu.

0006-3495/01/02/755/10 $2.00

nal concentration far below their extracellular concentration (i.e., do not achieve equilibrium), and 4) as cell density increases, electroporation applied at the same bulk field strength causes diminished effects due to local perturbation of the electric field by neighboring cells.

MATERIALS AND METHODS

Cell preparation

DU 145 prostate cancer cells were obtained from American Type Culture Collection (Rockville, MD) and grown as a monolayer in a 5% CO_2 and 37°C environment in RPMI-1640 medium with 0.3 g/L L-glutamine, 10% (v/v) heat-inactivated fetal bovine serum, 100 U/ml penicillin, 100 μg/ml streptomycin, and 250 μg/ml amphotericin B (Sigma Chemical Co., St. Louis, MO). The cells were harvested during the exponential growth phase using 0.1% trypsin-EDTA (Sigma).

Electroporation protocol

After harvesting, cell concentration in the growth media was determined using a hemacytometer (Hausser Scientific, Horsham, PA). Cells were then spun down ($1000 \times g$, 5 min; GS-15R, Beckman, Palo Alto, CA) and resuspended between 1×10^6 and 4×10^7 cells/ml in RPMI-1640 containing 25 mM HEPES buffer (Sigma) and 10^{-5} to 10^{-3} M calcein (623 Da, $z = -4$; lot 2532–5, Molecular Probes, Eugene, OR).

Electroporation was performed at room temperature (22 ± 1°C) by introducing 0.4 ml of cell suspension into a 2-mm gap cuvette with parallel-plate aluminum electrodes (BTX, San Diego, CA). Cuvettes were washed and reused up to five times. Exponential decay pulses (Electro Cell Manipulator 600, BTX) were applied using different pulse lengths (i.e., exponential decay time constants, 0.05–20 ms), field strengths (0.1–3.3 kV/cm), and numbers of pulses (1–10). An inter-pulse spacing of 20 s was used for multiple pulse experiments. For microsecond-scale pulses, resistors (Ohmite, Skokie, IL) were placed in parallel with the cuvette chamber to decrease the pulse length to the desired time constant.

After pulsing, cells were incubated at 37°C for 10 min in a water bath (Isotemp 210, Fisher Scientific, Pittsburgh, PA) and then washed twice by spinning down ($735 \times g$, 3 min; Eppendorf 5415 C, Brinkman, Westbury, NY) and resuspending the cell pellet with Dulbecco's phosphate-buffered saline free of magnesium and calcium (Mediatech, Herndon, VA). To assess cell viability, 10 μg/ml of the viability stain propidium iodide (Molecular Probes) (Shapiro, 1988) and 10^5/ml fluorescent latex microspheres ($d = 6$ μm; Polysciences, Warrington, PA) were added to each sample before storage on ice until analysis the same day. Propidium iodide stains nonviable cells red. The microspheres were used as an internal volumetric standard for determining cell concentration to account for cells destroyed during the electroporation process (Prausnitz et al., 1993).

Heating due to a pulse was less than 10°C for almost all (>98%) of the conditions used in this study. A pulse rise of 10°C increases the temperature from room temperature (~22°C) to ~32°C, which is less than the post-pulse incubation temperature of 37°C. Thus, samples pulsed at conditions generating a lot of heat were rapidly heated, for example, from 22°C to 32°C and then slowly heated to 37°C in the incubation bath, while unpulsed controls were slowly heated from 22°C to 37°C. Although the time scales of heating were not the same, control samples accounted for effects of heating, if there were any. Previous work suggests that temperature at the time of pulsing (0°C, 25°C, or 37°C) has little effect on uptake (Prausnitz et al., 1994).

Flow cytometry measurements

A FACSort flow cytometer (Becton Dickinson, Franklin Lakes, NJ) using LYSIS II software performed individual measurements on cells and microspheres. At least 10,000 viable cells were measured from each sample at a rate of up to 1000 cells/s. The samples were excited using the 488-nm line of an argon laser (Innova, Coherent, Palo Alto, CA). As shown in Fig. 1, *A* and *C*, light-scatter and fluorescence measurements were used as an indication of object size and shape, allowing discrimination between cells, microspheres, and debris. Propidium iodide fluorescence (677-nm longpass filter) was used to distinguish between viable and nonviable cells (Fig. 1 *B*). Flow cytometry data were stored on a personal computer (Lanier Micro, Gainesville, GA) and later analyzed using Windows Multiple Document Interface software (WinMDI, La Jolla, CA). No spectral compensation was necessary because there was not significant overlap of the propidium iodide signal into the calcein channel.

Quantitative fluorescence calibration

Viable cells were analyzed to determine the mean calcein fluorescence intensity (green) (530/30-nm bandpass filter). Representative histograms from a control sample and electroporated sample are shown in Fig. 1, *D* and *E*, respectively. To reduce the influence of outliers when calculating the mean, the brightest 3% of each population was not included. The mean fluorescence was then converted into the average number of calcein molecules inside each cell using quantitative calibration beads that fluoresce with an intensity equivalent to known numbers of free fluorescein molecules in solution, (Flow Cytometry Standards Corp, San Juan, PR) as described previously (Prausnitz et al., 1993). This calculation was facilitated by determining the ratio of the fluorescence of free calcein to free fluorescein using a spectrofluorimeter (Photon Technology International, South Brunswick, NJ) (Prausnitz et al., 1993). This intensity ratio was determined to be 0.86 ± 0.11 for the fluorescein (lot 26H3407; Sigma) and calcein used.

Calcein is an established tracer molecule that is unable to cross intact cell membranes and fluoresces independently of pH (6.5–9.5) (Haughland, 1992). Therefore any fluorescence associated with control samples should be due to cell autofluorescence, surface binding of calcein and/or flow cytometer electrical and optical noise. Fluorescence of electroporated samples was visually verified to be intracellular and not due to surface binding using fluorescence microscopy (IX70 with IX-FLA attachment, Olympus, Lake Success, NY) and laser scanning confocal microscopy (LSM 510, Carl Zeiss, Thornwood, NY). Therefore the number of molecules taken up per cell has been calculated by subtracting the fluorescence of control samples from that of electroporated samples. For samples that were brighter than the fluorescence calibration bead range, a second set of higher intensity fluorescent beads (LinearFlow Green beads, lot 5861, Molecular Probes) was used, after being calibrated by us with the spectrofluorimeter. Extrapolation of the calibration curves yielded by the low-intensity and high-intensity beads provided approximately overlapping lines (data not shown), showing that fluorescence intensity and calcein concentration correlated linearly over the full range of intensities encountered in this study.

The relationship between the extracellular and intracellular calcein concentration is expressed as the percent external concentration, which was calculated by dividing the final intracellular concentration by the initial extracellular concentration. The intracellular concentration was determined based on a cell diameter of 22 μm, as estimated microscopically using a hemacytometer as a ruler and in agreement with previous observations (Essand et al., 1995). Variation in cell diameter was estimated by microscopy to be a few microns (data not shown). This yields a volume of 5.6×10^{-9} ml per cell, assuming a spherical shape. We assumed that the initial and final extracellular concentrations were the same, because for 10^6 cells/ml (the cell concentration typically used) and the maximum cellular uptake (i.e., if the intracellular concentration equaled the initial extracellular concentration), the extracellular concentration would be diminished by less than 1%. For larger cell concentrations (i.e., 23% cells by volume) the greatest levels of uptake achieved were much less than 10% of the

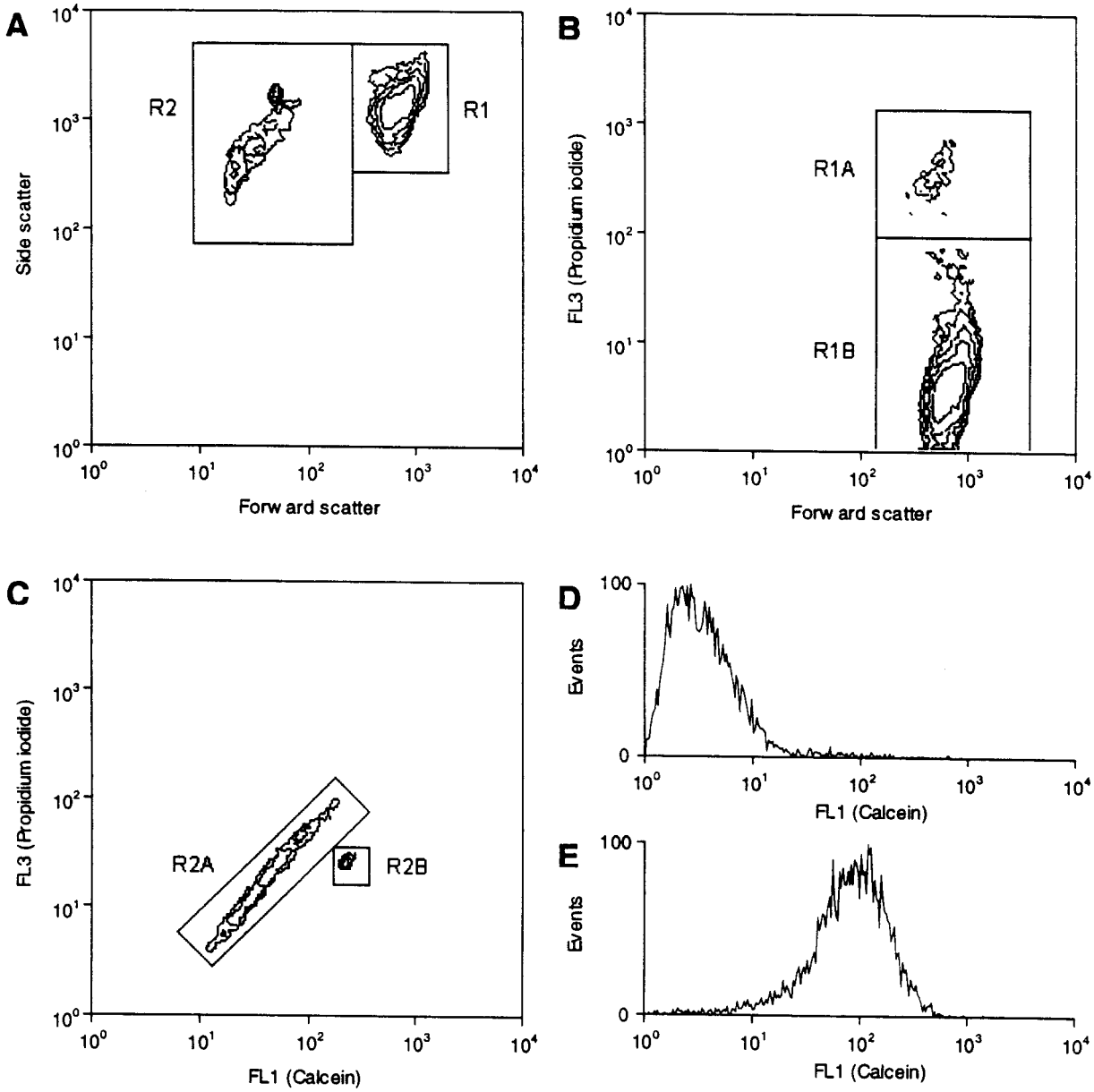

FIGURE 1 Typical flow cytometry contour and histogram plots that show how data were analyzed to yield number of molecules taken up per cell and percent of cells viable. (*A*) Light scatter was used to distinguish cells (R1) from microspheres and debris (R2). (*B*) Propidium iodide fluorescence separates nonviable cells (R1A) from viable cells (R1B; the population used for analysis) gated on R1. (*C*) Red and green fluorescence were used to separate microspheres (R2B; used for calibration of cell concentration) from debris (R2A) gated on R2. (*D*) Calcein histogram for a nonelectroporated control sample gated on R1B. (*E*) Calcein histogram for electroporated sample (0.55 kV/cm, 10.3 ms) gated on R1B. The number of molecules taken up per cell is determined by converting the average fluorescence shown on plot *E* into number of calcein molecules using calibrated beads (see text) and subtracting the converted average fluorescence shown for a control sample in plot *D*. The percent of cells viable is determined by calculating the number of viable cells (population R1B) per milliliter (determined based on the number of latex beads, population R2B) and dividing it by the number of viable cells per milliliter in control samples.

external concentration. This leads to a maximum external concentration depletion of 3%, which was not considered significant.

Viability was calculated by normalizing the non-electroporated controls to have 100% viability. The ratio of the concentration of the recovered viable cells (determined using the latex beads) to that of controls was then used to determine the viability.

Electric field determination

The applied voltage, pulse length, and current were measured using an oscilloscope (54602B, Hewlett Packard) and a current monitor (411, Pearson Electronics, Palo Alto, CA). By measuring cell suspension conductivity (1.29 S/m at 25°C; model 32, YSI, Yellow Springs, OH), electrode

spacing (0.2 ± 0.01 cm) and solution volume (0.4 ml), we determined the solution resistance (7.8 Ω) (Serway, 1990). Assuming suspension resistance was independent of field strength, we then used Ohm's law along with the suspension resistance, electrode spacing, and the measured current to determine the field strength within the cuvette for each experiment. This method should yield a more accurate field strength than the nominal field strength determined by dividing the applied voltage by the electrode spacing, because significant voltage drops can occur at the electrode-solution interface (Pliquett et al., 1996). Using this method, actual fields were found in this study to be approximately 90% of the nominal field strength (data not shown).

The pre-electroporation transmembrane potential, Ψ, was determined using Eq. 1 (Foster and Schwann, 1986), which models non-electroporated cells as insulating spheres:

$$\Psi = 1.5Ur\cos\theta, \tag{1}$$

where r is the cell radius, U is the bulk field strength, and θ is the angle from the poles. Assuming a spherical shape, for 10^6 cells/ml the volume percentage occupied by cells is 0.6%. At this concentration, cells should be sufficiently far apart from one another that they do not locally alter the electric field experienced by neighboring cells based on the analysis by Susil et al. (1998), for $R = I/d = 3.5$, where I is the cell-cell spacing and d is the cell diameter.

At denser concentrations, neighboring cells can influence each other, as discussed in Results. To account for the electric field perturbation caused by neighboring cells, a function was fitted to the simulation output data from Susil et al. (1998) at the maximum transmembrane potential ($\theta = 0$) to yield a corrected maximum transmembrane potential, Ψ_c:

$$\Psi_c = 1.5Ur\left[1 - \frac{e^{(-2.5R^{0.9})}}{3}\right] \tag{2}$$

$$R = [(x^{-1/3}) - d]/d, \tag{3}$$

where x is the cell concentration (e.g., cells/ml) and $1/x$ is the characteristic volume occupied by a cell (e.g., ml/cell) and its surrounding solvent. This volume can be described as a cube of characteristic length $x^{-1/3} = d + I$.

RESULTS

Population responses

Using two-color flow cytometry, electroporation-mediated molecular uptake and cell viability were analyzed for thousands of individual DU 145 prostate cancer cells exposed to one of more than 200 experimental conditions. Calcein, a model cell-impermeant, green-fluorescent tracer compound, was used as the molecular transport marker. The absolute number of calcein molecules transported into each cell was calculated using calibrated beads. Propidium iodide, a red-fluorescent viability stain, was used to identify nonviable cells.

Fig. 1, *D* and *E*, show a representative increase in green fluorescence of viable cells upon electroporation. The fluorescence of the nonpulsed, control population (Fig. 1 *D*) was due to autofluorescence, calcein surface binding, and flow cytometer electrical and optical noise. The nearly two-orders-of-magnitude increase in fluorescence seen for pulsed cells (Fig. 1 *E*) indicates significant uptake of exogenous calcein molecules. It should be noted that despite the broad distributions, a single population was observed in each sample. This uniform population response allowed the use of the average intensity to be representative of the population.

Field strength, pulse length, and pulse number

To understand the interacting effects of pulse field strength, length, and number, DU 145 cells were electroporated using a broad range of different electrical conditions. Fig. 2 shows uptake of calcein (left column) and cell viability (right column) as a function of field strength and pulse length for between 1 pulse (top row) and 10 pulses (bottom row). Each graph has a family of curves, each representing different pulse lengths. The data points represent experimental data, whereas the continuous curves are generated from a statistical correlation described elsewhere (P. J. Canatella and M. R. Prausnitz, submitted for publication) and presented to aid the reader to visually group data points. Fig. 3 shows the same set of data re-plotted so that each graph is for a given pulse length between 50 μs (top row) and 10 ms (bottom row), and families of curves for different numbers of pulses are shown. Because exponential decay pulses were used, the term pulse length refers here to the exponential decay time constant of the pulse.

Figs. 2 and 3 show the dependence of uptake and viability on field strength. At a given pulse length and number (i.e., along any one curve in Fig. 2 or 3), uptake was indistinguishable from control samples below a quasi-threshold field strength. Uptake then increases with increasing field strength and in some cases may begin to plateau at high field strengths. The dependence of viability on field strength shows similar behavior; above a quasi-threshold, viability decreases with increasing field strength and (although not apparent from these data) must level off close to zero viability at high field strengths.

The dependence of uptake and viability on pulse length (Fig. 2) and number of pulses (Fig. 3) is also shown. For uptake, increasing pulse length or number amplified the effects of field strength by reducing the quasi-threshold field strength, increasing the slope of the field strength dependence, and possibly raising the plateau level. Likewise for viability, the pulse length and number amplified the effects of field strength by reducing the quasi-threshold field strength and increasing the slope of the field strength dependence, which caused the viability to approach zero at smaller field strengths.

Many of the conditions shown in Figs. 2 and 3 indicate that uptake of large numbers of molecules is often accompanied by large loss of cell viability. To describe the net effect of electroporation, the product of uptake and viability can be used as a measure of the total number of molecules delivered into the entire population of viable cells. As shown in Fig. 4, an initial increase in this quantity is seen due to the increase in molecular transport with increasing field strength. A peak value is then seen where the greatest

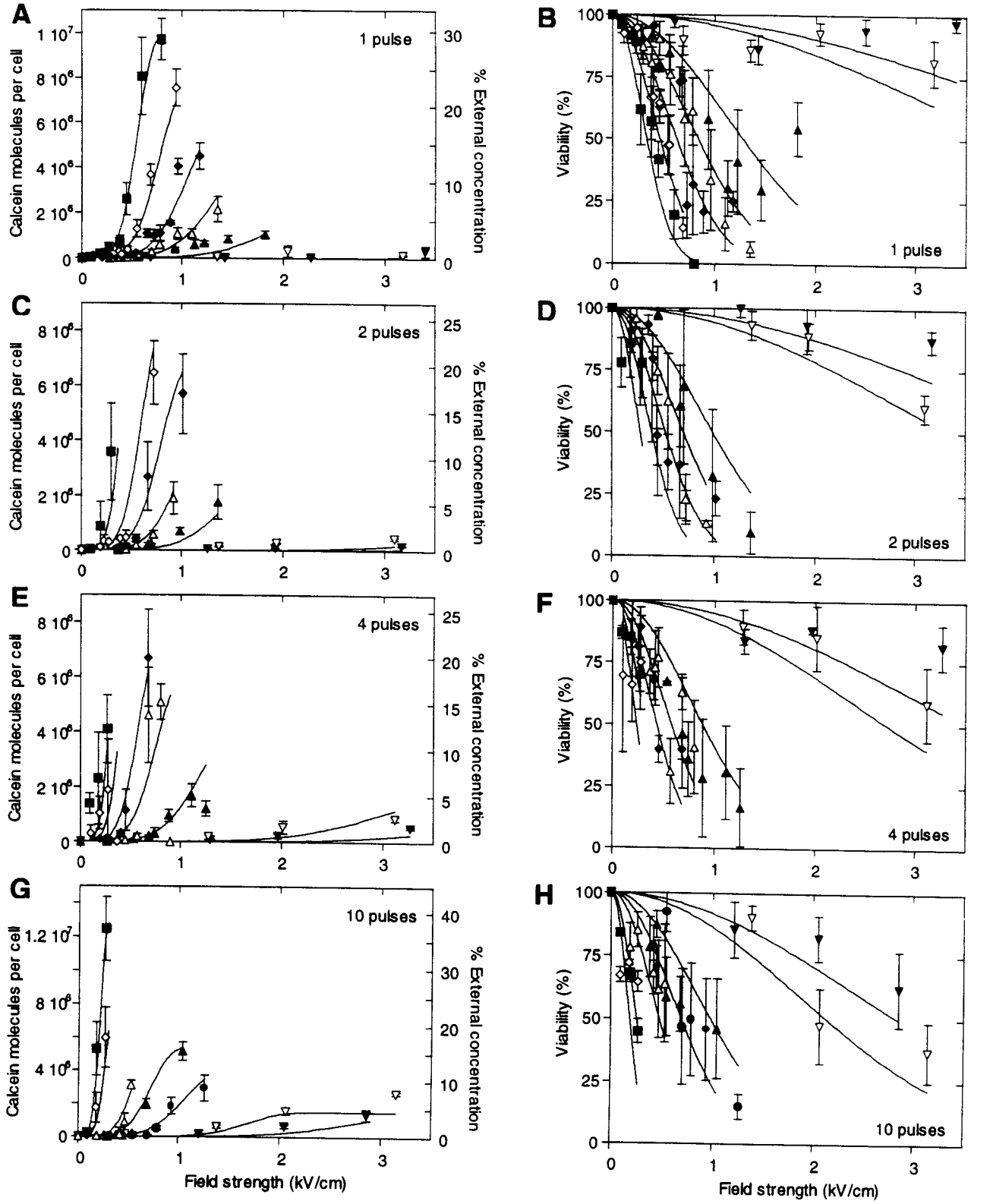

FIGURE 2 Uptake and viability dependence on field strength and pulse length for different number of pulses. Either 1 (*A* and *B*), 2 (*C* and *D*), 4 (*E* and *F*), or 10 (*G* and *H*) pulses were applied at pulse lengths of 0.050 ± 0.004 (▼), 0.090 ± 0.006 (▽), 0.50 ± 0.09 (●), 1.1 ± 0.2 (▲), 2.8 ± 0.5 (△), 5.3 ± 0.5 (♦), 10 ± 1 (◇), and 21 ± 2 ms (■). Data points represent the average of between three and nine samples collected at 10^{-5} M calcein and 10^6 cells/ml. Curves are generated from a statistical correlation (P. J. Canatella and M. R. Prausnitz, submitted for publication) to aid viewing the figure.

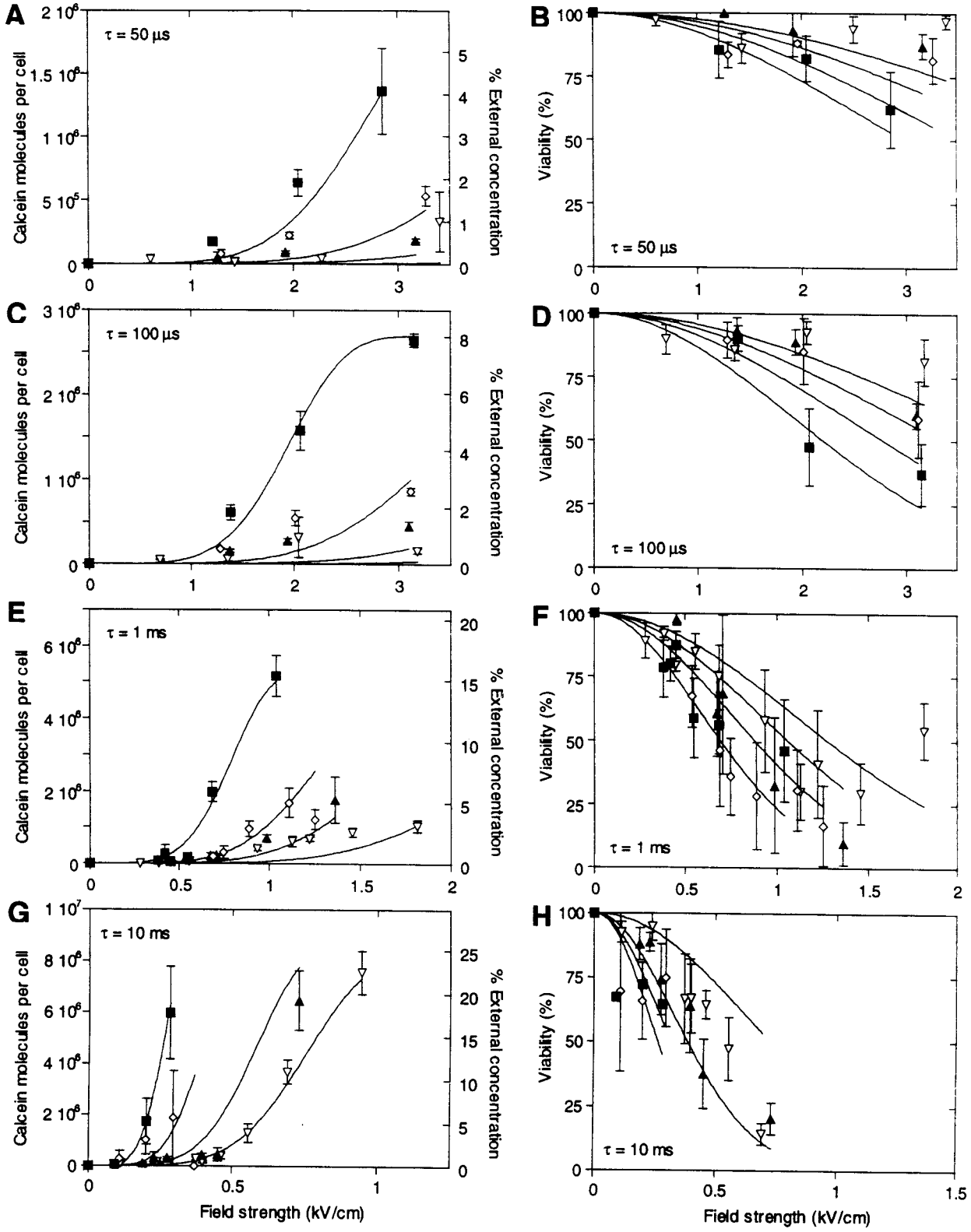

FIGURE 3 Dependence of calcein uptake and cell viability on field strength and number of pulses for different pulse lengths. The pulse length was either 0.050 ± 0.004 (*A* and *B*), 0.090 ± 0.006 (*C* and *D*), 1.1 ± 0.2 (*E* and *F*), or 10 ± 1 (*G* and *H*) ms with either 1 (▽), 2 (▲), 4 (◇), or 10 (■) pulses. This figure contains the same data plotted in Fig. 2. Curves are generated from a statistical correlation (P. J. Canatella and M. R. Prausnitz, submitted for publication) to aid viewing the figure.

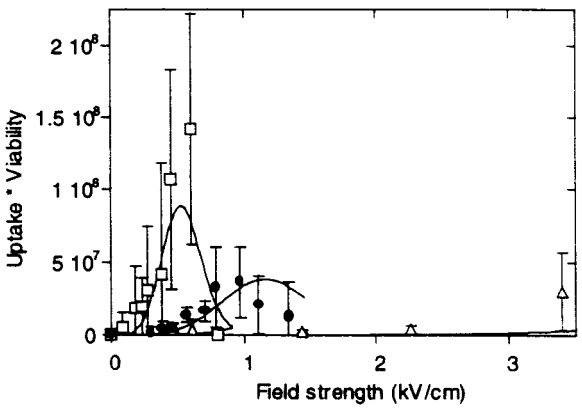

FIGURE 4 Dependence of the product of uptake and viability on field strength, pulse length, and number of pulses. A single pulse was applied at pulse lengths of 0.055 ± 0.007 (△), 3.2 ± 0.2 (●), and 22 ± 1 ms (□). Data points represent the average of between three and six samples collected at 10^{-5} M calcein and 10^6 cells/ml. Curves are generated from a statistical correlation (P. J. Canatella and M. R. Prausnitz, submitted for publication) to aid viewing the figure.

numbers of molecules are in the greatest number of viable cells. This is followed by a decrease due to the loss of viability with increasing field strength. The peak conditions seen based on this presentation of the data may correspond to optimal electroporation conditions for some applications.

Cell and calcein concentration

In addition to the effects of electrical conditions, we also examined the effects of cell and solute (i.e., calcein) concentration on uptake and viability. The effect of cell concentration is shown in Fig. 5. Increasing cell concentration is shown to decrease uptake (Fig. 5 *A*) and may increase viability (Fig. 5 *B*). This reduced effect of electroporation at dense cell concentrations could be explained by local perturbation of the electric field caused by neighboring cells. As described in Materials and Methods, the calculations of Susil et al. (1998) were used to determine the local electric field experienced by a cell based on the bulk electric field and cell density. When the data are re-plotted using the

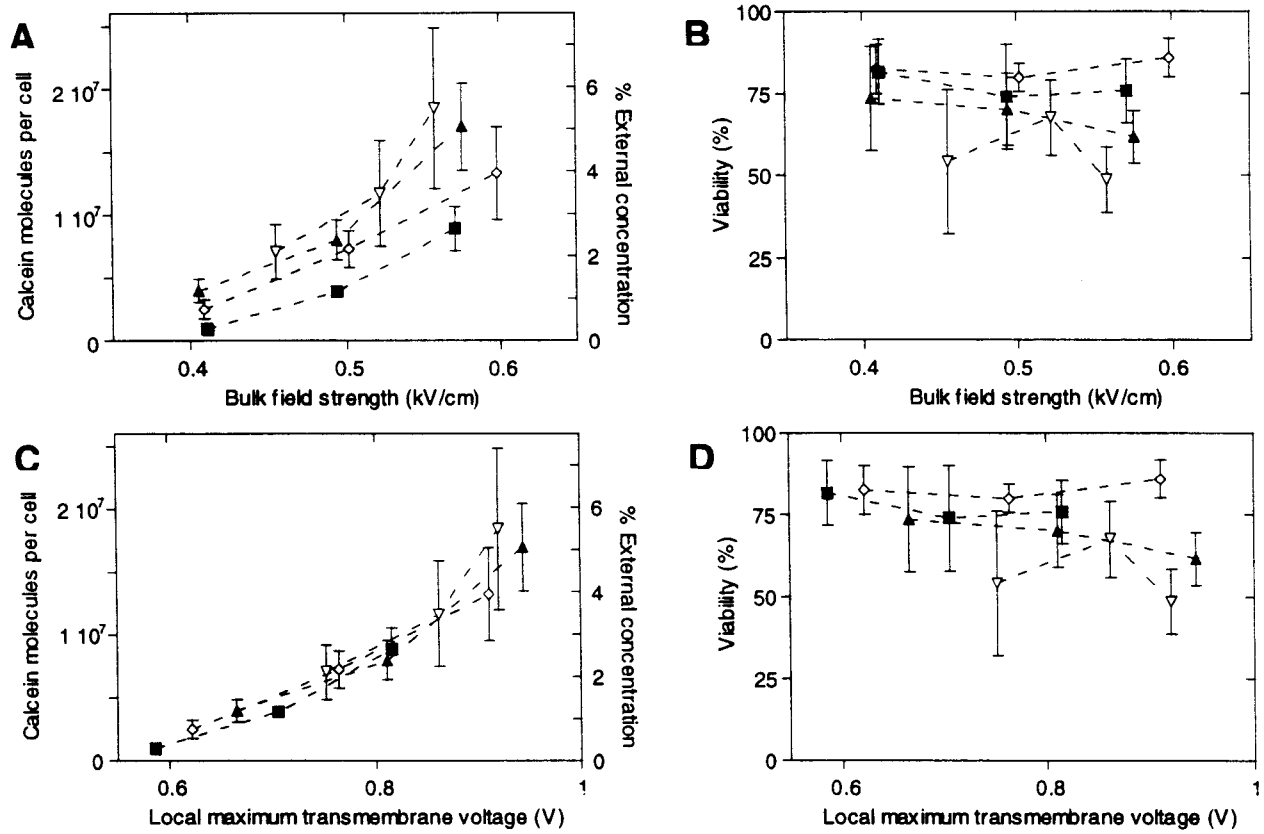

FIGURE 5 Dependence of molecular uptake and cell viability on cell concentration. The cell concentrations used were 1×10^6 (▽), 5×10^6 (▲), 25×10^6 (◇), and 40×10^6 (■) cells/ml. Increased cell concentration appears to decrease uptake (*A*) and possibly increase viability (*B*) when comparisons are made using the nominal bulk electric field (data points are connected for clarity). After re-plotting the same data and correcting the electric field for neighboring cell effects (see text), the uptake (*C*) and viability (*D*) data points collapse into a single curve. The *x* axis provides the local maximum transmembrane voltage (V/membrane), rather than the bulk field strength (kV/cm). All data points represent the average of between three and seven samples. All samples were electroporated with a single pulse of 10.1 ± 1.1 ms and 10^{-4} M calcein.

corrected local electric field as the *x* axis (Fig. 5, *C* and *D*), the family of curves collapse into a single curve, which suggests that the dominant effect of increasing cell density is reduction of the local field experienced by a cell. This observation shows that electric field perturbations are an important factor to consider, among others, for electroporation of cells at high density within tissues, such as in electrochemotherapy.

Fig. 6 *A* shows that uptake of calcein scaled directly with extracellular calcein concentration; at the conditions tested, intracellular calcein concentration was always approximately 2% of the external concentration (Tukey's multiple comparison, $p = 0.865$). Fig. 6 *B* shows that calcein concentration did not affect cell viability ($p = 0.308$), as would be expected for an inert marker compound.

Applied charge and energy

Some previous studies have suggested that uptake and/or viability depend on electrical charge (Liang et al., 1988; Prausnitz et al., 1994) or energy (Kubiniec et al., 1990; Neumann et al., 1998). Because these studies had much smaller data sets, we used the large data set presented here to test for possible correlation between charge or energy with uptake and viability (Fig. 7). Fig. 7, *A* and *B*, shows that, in general, transport increases and viability decreases with charge (*C*). However, a simple dependence (e.g., linear correlation) on charge does not appear to exist for either uptake ($N = 9.3 \times 10^6 C + 52{,}000$; $R^2 = 0.519$; $F = 6.03$) or viability ($V = -32C + 67$; $R^2 = 0.032$; $F = 3.81$). The applied energy (*J*) was also examined (Fig. 7, *C* and *D*). Although a somewhat better predictor than charge, the linear correlations for energy are also poor for both uptake ($N = 2.7 \times 10^5 J - 6.3 \times 10^5$; $R^2 = 0.679$; $F = 3.21$) and viability ($V = -2.3J + 79$; $R^2 = 0.252$; $F = 2.38$). This indicates that neither charge nor energy predicts uptake or viability well and that more complex functionalities are needed.

DISCUSSION

Hypotheses 1 and 2

The data collected in this study quantitatively show the dependence of uptake and viability on electrical parameters. Previous studies have proposed that charge (i.e., $U\tau n$) was a good predictor of uptake (Liang et al., 1988; Prausnitz et al., 1994). This could be consistent with transport by electrophoresis, where some fraction of the charge moved across the membrane would be carried by calcein molecules. However, in this study, the charge delivered was a poor predictor of uptake and an even worse predictor of cell viability (Fig. 7, *A* and *B*), suggesting that hypothesis 1, as proposed in the Introduction, is incorrect. Energy (i.e., $U^2\tau n$) has also been used to model transport (Kubiniec et al., 1990; Neumann et al., 1998), which could be consistent with transport limited by the number of pores created, which is thought to be an energy-dependent phenomenon (Chang et al., 1992). This study showed that energy was also a poor descriptor of transport and viability (Fig. 7, *C* and *D*), suggesting that hypothesis 2 is incorrect. A more complex dependence on electrical parameters is warranted because uptake and viability depend on the interactive effects of pore creation, growth, and resealing; transport by electrophoresis, electro-osmosis, and diffusion; and other effects.

Hypothesis 3

Experimental measurements in this study never showed the intracellular concentration reaching the extracellular con-

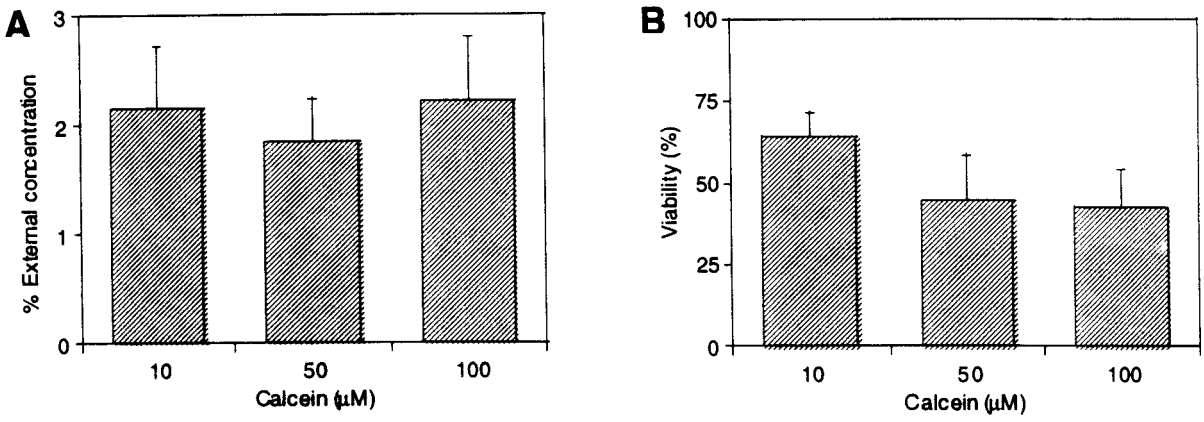

FIGURE 6 Uptake and viability dependence on calcein concentration. (*A*) Uptake is shown to scale directly with solute concentration because the ratio of the internal to external concentration (i.e., percent external concentration) remained constant (Tukey's multiple comparison, $p = 0.865$). (*B*) Viability is not affected by calcein concentration ($p = 0.308$). All data points represent the average of between three and seven samples. All samples were pulsed with a single pulse of 0.48 ± 0.04 kV/cm for 10.9 ± 0.5 ms.

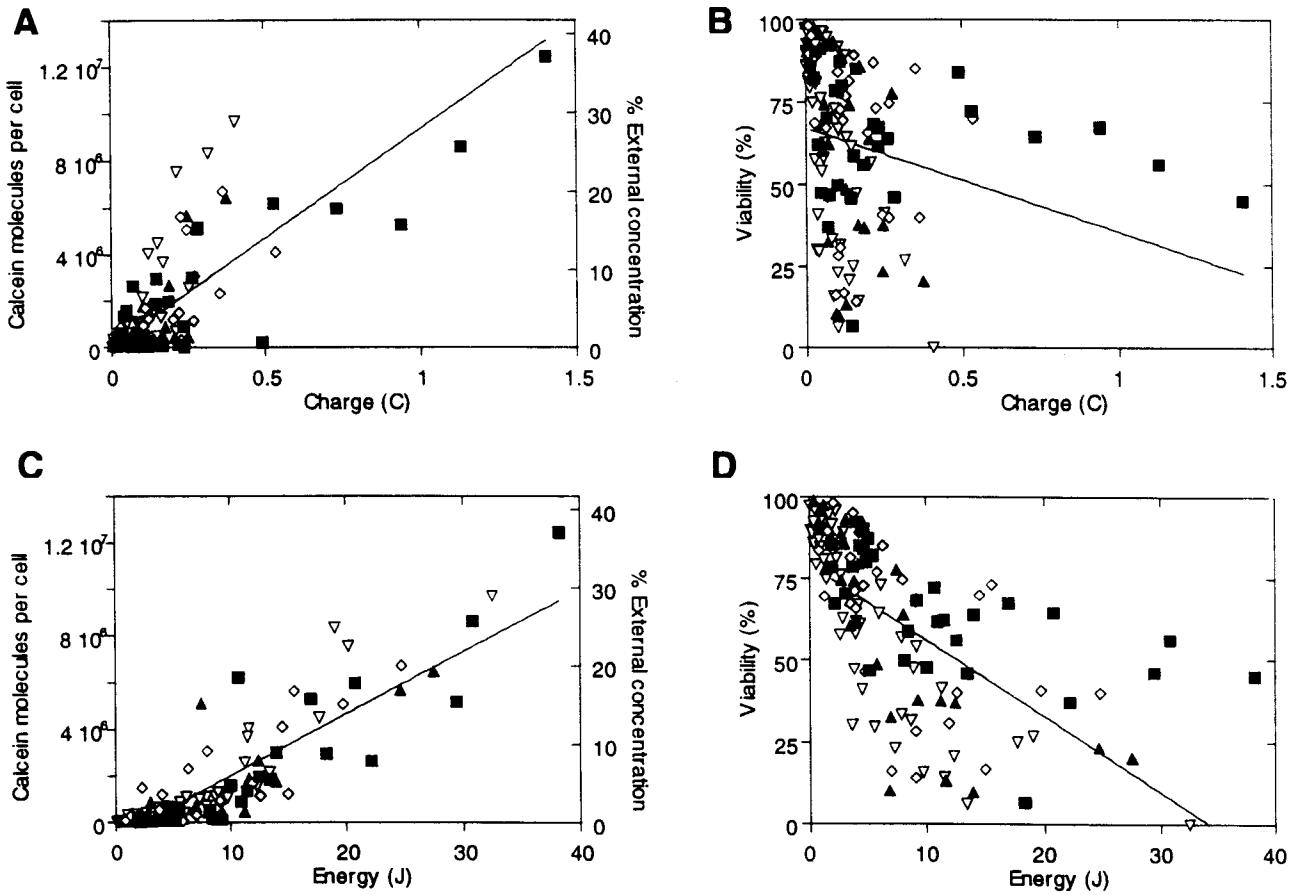

FIGURE 7 Dependence of calcein uptake and cell viability on electroporation pulse charge and energy. The approximately 200 different pulse conditions shown in Figs. 2–5 were used with field strengths ranging from 0.1 to 3.3 kV/cm and pulse lengths from 0.05 to 20 ms. Either 1 (▽), 2 (▲), 4 (◇), or 10 (■) pulses were applied. Uptake and viability did not show a good linear correlation with either charge ($R^2 = 0.519$ and $R^2 = 0.032$, respectively) or energy ($R^2 = 0.679$ and $R^2 = 0.252$, respectively). Data points represent the average of between three and nine samples collected at 10^{-5} M calcein and 10^6 cells/ml. Charge (and energy) were calculated assuming a constant bulk resistance.

centration of calcein, suggesting a non-equilibrium condition. The intracellular concentration was at most 37% of the extracellular concentration and was usually much less. This finding supports hypothesis 3 and is in agreement with previous studies with red blood cell ghosts (Prausnitz et al., 1993), yeast cells (Gift and Weaver, 1995), and mammalian cells (Bazille et al., 1989) but not in agreement with DeLeo et al. (1996) who obtained 100% of initial extracellular concentration when delivering proteins into neutrophils.

Intracellular concentrations that appear lower than extracellular concentrations could be explained by excluded volume within cells; i.e., the actual cell volume is less than expected. However, examination by confocal microscopy showed that calcein was distributed throughout the entire cell (data not shown) suggesting that sub-equilibrium is not due to an excluded volume.

Another explanation for sub-equilibrium uptake could involve saturation of intracellular binding sites. This is unlikely, because calcein is not expected to bind to cells. Moreover, Fig. 6 shows that uptake scaled directly with external calcein concentration, indicating a saturation of electroporation's effect on uptake rather than a saturation of binding sites. Finally, we incubated cells in calcein AM, a modified form of calcein that freely enters cells, but once inside a cell is enzymatically modified back into calcein and thereby trapped within the cell. Calcein-AM-loaded cells had an intracellular concentration significantly greater than those achieved by electroporation (data not shown) and corresponded to 95% of the extracellular concentration, indicating that more calcein could enter the cells and thus electroporation caused only sub-equilibrium transport.

Hypothesis 4

As cell density increased, molecular uptake and loss of viability decreased for the same bulk electroporation conditions (Fig. 5). By accounting for local perturbation of the

electric field by neighboring cells, these effects of cell density were explained, in support of hypothesis 4. This demonstrates the importance of determining the correct local electric field experienced by a cell, rather than relying on bulk values.

CONCLUSIONS

A comprehensive set of data was collected at more than 200 different electroporation conditions. The intracellular calcein concentration levels achieved in this study were at most 37% of the extracellular concentration, indicating a subequilibrium condition. Cell concentration effects were accounted for by correcting for disturbances in the field by neighboring cells. Uptake was shown to have a linear dependence on calcein concentration over the range tested. Direct correlation of data with applied charge and energy were shown to be poor predictors of uptake and viability. These data should provide a tool to develop and validate mechanistic insight and a guide to optimize electroporation protocols.

We thank Robert Karaffa for help with flow cytometry, Dr. Russell Heikes for help with statistical analysis and Susannah Smith, Donald Betah, and Esi Ghartey-Tagoe for technical assistance.

This work was supported in part by a National Science Foundation CAREER award and the Emory/Georgia Tech Biomedical Technology Research Center.

REFERENCES

Bartoletti, D. C., G. I. Harrison, and J. C. Weaver. 1989. The number of molecules taken up by electroporated cells: quantitative determination. *FEBS Lett.* 256:4–10.

Bazille, D., L. M. Mir, and C. Paoletti. 1989. Voltage-dependent introduction of a d[α]octothymidylate into electropermeabilized cells. *Biochem. Biophys. Res. Commun.* 159:633–639.

Chang, D. C., B. M. Chassy, J. A. Saunders, and A. E. Sowers (editors). 1992. Guide to Electroporation and Electrofusion. Academic Press, New York.

DeLeo, F. R., M. A. Jutila, and M. T. Quinn. 1996. Characterization of peptide diffusion into electropermeabilized neutrophils. *J. Immunol. Methods.* 198:35–49.

Essand, M., Grönvik, C., T. Hartman, and J. Carlsson. 1995. Radioimmunotherapy of prostatic adenocarcinomas: effects of ^{131}I-labelled E4 antibodies on cells at different depth in DU 145 spheroids. *Int. J. Cancer.* 63:387–394.

Foster, K. R., and H. P. Schwann. 1986. Dielectric properties of tissues. *In* CRC Handbook of Biological Effects of Electromagnetic Fields. C. Polk. and E. Postow, editors. CRC Press, Boca Raton, FL.

Gift, E. A., and J. C. Weaver. 1995. Observation of extremely heterogeneous electroporative molecular uptake by *Saccharomyces cervisiae* which changes with electric field pulse amplitude. *Biochim. Biophys. Acta.* 1234:52–62.

Haughland, R. P. 1992. Handbook of Fluorescent Probes and Research Chemicals. Molecular Probes, Eugene, OR.

Heller, R., R. Gilbert, and M. J. Jaroszeski. 1999. Clinical applications of drug delivery. *Adv. Drug Del. Rev.* 35:119–129.

Kubiniec, R. T., H. Liang, and S. W. Hui. 1990. Effects of pulse length and pulse strength on transfection by electroporation. *BioTechniques.* 8:16–20.

Liang, H., W. J. Purucker, D. A. Stenger, R. T. Kubiniec, and S. W. Hui. 1988. Uptake of fluorescence-labeled dextrans by 10T 1/2 fibroblasts following permeation by rectangular and exponential-decay electric field pulses. *BioTechniques.* 6:550–558.

Lynch, P. T., and M. R. Davey. 1996. Electrical Manipulation of Cells. Chapman and Hall, New York.

Mir, L. M., and S. Orlowski. 1999. Mechanisms of electrochemotherapy. *Adv. Drug Deliv. Rev.* 35:107–118.

Neumann, E., A. E. Sowers, and C. A. Jordan. 1989. Electroporation and Electrofusion in Cell Biology. Plenum Press, New York.

Neumann, E., K. Toensing, S. Kakorin, P. Budde, and J. Frey. 1998. Mechanism of electroporative dye uptake by mouse B cells. *Biophys. J.* 74:98–108.

Nickoloff, J. A. 1995. Animal Cell Electroporation and Electrofusion Protocols. Humana Press, Totowa, NJ.

Pliquett, U., E. A. Gift, and J. C. Weaver. 1996. Determination of the electric field and anomalous heating caused by exponential pulses with aluminum electrodes in electroporation experiments. *Bioelectrochem. Bioenerg.* 39:39–53.

Prausnitz, M. R., B. S. Lau, C. D. Milano, S. Conner, R. Langer, and J. C. Weaver. 1993. A quantitative study of electroporation showing a plateau in net molecular transport. *Biophys. J.* 65:414–422.

Prausnitz, M. R., C. D. Milano, J. A. Gimm, R. Langer, and J. C. Weaver. 1994. Quantitative study of molecular transport due to electroporation: uptake of bovine serum albumin by erythrocyte ghosts. *Biophys. J.* 66:1522–1530.

Rols, M., and J. Teissie. 1990. Electropermeabilization of mammalian cells: quantitative analysis of the phenomenon. *Biophys. J.* 58: 1089–1098.

Serway, R. 1990. Physics for Scientists and Engineers. Saunders College Publishing, Philadelphia.

Shapiro, H. M. 1988. Practical Flow Cytometry. Alan R. Liss, New York.

Susil, R., D. Semrov, and D. Miklavcic. 1998. Electric field-induced transmembrane potential depends on cell density and organization. *Electro. Magnetobiol.*. 17:391–399.